**R. F. Turchiello[1]\***
**M. T. Lamy-Freund[1]**
**I. Y. Hirata[2]**
**L. Juliano[2]**
**A. S. Ito[3]**

[1] *Instituto de Fisica, Universidade de São Paulo, Brasil*

[2] *Departamento de Biofisica, Universidade Federal de São Paulo, Brasil*

[3] *Departmento de Física e Matemática, Faculdade de Filosofia Ciências e Letras de Ribeirão Preto, Universidade de São Paulo, Av. Bandeirantes 3900, 14040-901, Ribeirão Preto, Brasil*

# Ortho-Aminobenzoic Acid-Labeled Bradykinins in Interaction with Lipid Vesicles: Fluorescence Study

**Abstract:** *The peptide hormone bradykinin (BK) ($Arg^1$-$Pro^2$-$Pro^3$-$Gly^4$-$Phe^5$-$Ser^6$-$Pro^7$-$Phe^8$-$Arg^9$) and its shorter homolog $BK^{1-5}$ ($Arg^1$-$Pro^2$-$Pro^3$-$Gly^4$-$Phe^5$) were labeled with the extrinsic fluorescent probe* ortho-*aminobenzoic acid (Abz) bound to the N-terminal and amidated in the C-terminal carboxyl group (Abz-BK-$NH_2$ and Abz-$BK^{1-5}$-$NH_2$). The fragment des-$Arg^9$-BK was synthesized with the Abz fluorescent probe attached to the 3-amino group of 2,3-amino propionic acid (DAP), which positioned the Abz group at the C-terminal side of BK sequence, constituting the peptide des-$Arg^9$-BK-DAP(Abz)-$NH_2$. The spectral characteristics of the probe were similar in the three peptides, and their fluorescent properties were monitored to study the interaction of the peptides with anionic vesicles of dimyristoylphosphatidylglycerol (DMPG). Time-resolved fluorescence experiments showed that the fluorescence decay of the peptides was best described by double-exponential kinetics, with mean lifetimes values around 8.0 ns in buffer pH 7.4 that*

*increased about 10% in the presence of DMPG vesicles. About a 10-fold increase, compared with the values in aqueous solution, was observed in the steady-state anisotropy in the presence of vesicles. A similar increase was also observed for the rotational correlation times obtained from time-resolved anisotropy decay profiles, and related to the overall tumbling of the peptides. Equilibrium binding constants for the peptide–lipid interaction were examined monitoring anisotropy values in titration experiments and the electrostatic effects were evaluated through Gouy–Chapman potential calculations. Without corrections for electrostatic effects, the labeled fragment Abz-BK$^{1-5}$-NH$_2$ presented the major affinity for DMPG vesicles. Corrections for the changes in peptide concentration due to electrostatic interactions suggested higher affinity of the BK fragments to the hydrophobic phase of the bilayer.* © 2002 Wiley Periodicals, Inc. Biopolymers 65: 336–346, 2002

## INTRODUCTION

Bradykinin (BK) is a peptide hormone with the amino acid sequence Arg$^1$-Pro$^2$-Pro$^3$-Gly$^4$-Phe$^5$-Ser$^6$-Pro$^7$-Phe$^8$-Arg$^9$. It is involved in several physiological processes, including inflammation, vasodilation, pain, and symptoms associated with the common cold.[1–4] Two types of G-protein coupled receptors, B1 and B2, interact with BK and related kinins: While B2 mediates most of the BK actions, B1 recognizes and binds mostly to the BK fragment des-Arg$^9$-BK.[5,6] Previous studies using circular dichroism (CD) and nuclear magnetic resonance (NMR) showed that BK, in aqueous medium, has a large degree of structural flexibility,[7,8] but in organic solvents, or in the presence of amphiphilic aggregates, displayed some preferential folded conformation.[9–13] Recently, a study using electron spin resonance (ESR) spectroscopy of spin labels intercalated in the lipid bilayer demonstrated that BK and some of its fragments (des-Arg$^9$-BK, des-Arg$^1$-BK, and BK$^{1-5}$) interact with anionic vesicles of dimyristoylphosphatidylglycerol (DMPG).[14] Different spin label molecules, with the paramagnetic center at different depths of the hydrocarbon chain, indicated that BK and fragments penetrate the bilayer, making it less fluid in the lipid liquid crystal phase. In the gel phase, the peptides also decrease the bilayer fluidity, and it was found that BK displays a stronger interaction with the membrane when compared with the fragments. The experimental data were interpreted as a result of not only the presence or two positively charged Arg in BK, which would increase the local peptide concentration at the anionic vesicle surface, but also due to the occurrence of the hydrophobic residue Phe in positions 5 and 8 of the amino acid sequence. The results suggested that the peptide's biologic activity could be correlated with the extent of their interaction with vesicles, supporting the hypoth-

esis of an active role of the membrane as a catalyst for ligant–receptor interactions.[15,16]

Although BK has two fluorescent residues, Phe$^5$ and Phe$^8$, their short excitation wavelength, where high light scattering occurs, and their low quantum yield are the major drawbacks for the use of fluorescence spectroscopy in the study of this peptide. Reports in the literature were limited to monitoring the Phe fluorescence to obtain information about the interaction of BK with micelles of cerebroside sulfate, phosphatidylinositol, and sodium dodecyl sulfate.[17] Alternatively, *ortho*-aminobenzoic acid (Abz) has been proposed as an extrinsic fluorescent probe for peptides. Abz's high quantum yield, 0.6 in ethanol,[18] small size, a structure comparable to those of natural amino acids, and the possibility of connecting the molecule to the N$^\alpha$ amino group of peptides without any significant change in its spectroscopic characteristics[19] qualifies it as a good extrinsic fluorescent probe for peptides. The only exception was found with the Abz bound directly to proline, due to the formation of pyrrolobenzodiazepine-5, 11-dione.[20] Properties of Abz-labeled peptides were studied in aqueous medium and in the presence of sodium dodecyl sulfate (SDS) micelles.[21] Abz has also been used as a convenient donor group in peptide sequences that are substrates for proteolytic enzymes, forming a donor–acceptor pair with *N*-[2,4-dinitrophenyl]ethylenediamine (EDDnp).[22,23] More recently, the Abz–EDDnp pair was used to study the conformational dynamics of BK-related peptides using Förster resonance energy transfer (FRET).[24] From time-resolved fluorescence decay profiles, end-to-end distance distributions in water and in trifluoroethanol (TFE) were determined, showing that a larger number of conformational states are present in aqueous medium compared to the occurrence of just one folded conformation in equilibrium with one extended conformation stabilized in that organic solvent.[24]

Abz has low affinity for lipids and can be used as a probe to monitor the peptide lipid affinity. In the present work, we investigated the use of Abz to monitor the interaction of BK and some fragments with DMPG lipid vesicles, with the aim of investigating the importance of the lipid phase for the peptide–membrane receptor interaction, thinking about the possible consequences to the peptide's biologic activity. The peptides studied were the BK native sequence, Abz-BK-NH$_2$, and a fragment with charge $+1$, Abz-BK$^{1–5}$-NH2 (Abz-Arg$^1$-Pro$^2$-Pro$^3$-Gly$^4$-Phe$^5$-NH$_2$), both having the Abz probe bound to their N-terminal. Another fragment, des-Arg$^9$-BK-DAP(Abz)-NH$_2$, was studied, with net charge $+1$ and having the Abz probe bound close to the C-terminal, attached to the peptide through the diaminopropionic acid (DAP). The carboxy group of all peptides were amidated. This is the first report of a peptide having the extrinsic fluorescent probe, Abz, bound near to the C-terminal to monitor the peptide interaction with amphiphilic aggregates.

## MATERIALS AND METHODS

### Peptide Synthesis

All peptides were obtained in an automated bench-top simultaneous multiple solid-phase peptide synthesizer (PSSM 8 system from Shimadzu) using the solid-phase synthesis by the Fmoc procedure. The final deprotected peptides were purified by semipreparative high-performance liquid chromatography (HPLC) using an Econosil C-18 column (10 $\mu$m, 22.5 $\times$ 250 mm) and a two-solvent system: (1) trifluoroacetic acid (TFA)/H$_2$O (1:1000) and (2) TFA/acetonitrile (ACN)/H$_2$O (1:900:100). The column was eluted at a flow rate of 5 mL/min with a 10 (or 30)–50 (or 60)% gradient of solvent B over 30 or 45 minutes. Analytic HPLC was performed using a binary HPLC system from Shimadzu with an SPD-10AV Shimadzu uv-vis detector and a Shimadzu RF-535 fluorescence detector, coupled to an Ultrasphere C-18 column (5 $\mu$m, 4.6 $\times$ 150 mm) that was eluted with solvent systems A$_1$ (H$_3$PO$_4$/H$_2$O, 1:1000) and B$_1$ (ACN/H$_2$O/H$_3$PO$_4$, 900:100:1) at a flow rate of 1.7 mL/min and a 10–80% gradient of B$_1$ over 15 minutes. The HPLC column eluates were monitored by their absorbance at 220 nm and by fluorescence emission at 420 nm following excitation at 320 nm. The molecular weight and purity of synthesized peptides were checked by MALDI-TOF mass spectrometry (TofSpec-E, Micromass) and/or peptide sequencing using protein sequencer PPSQ-23 (Shimadzu, Tokyo, Japan).

### Materials

The sodium salt of the phospholipid DMPG (1,2-dimyristoyl-*sn*-glycero-3-phospho-*rac*-glycerol) was purchased from Avanti Polar Lipids (Birmingham, AL). The HEPES (4-(2-hydroxyethyl)-1-piperizineethanesulfonic acid) and SDS, used without additional purification, were obtained from Sigma Chemical Co. (St. Louis, MO). The HEPES buffer, adjusted with NaOH to pH 7.4, was used at 0.01$M$ concentration.

### Vesicles Preparation

Lipid vesicles were prepared by the method of extrusion[25] A lipid film was formed from a chloroform solution of lipids, dried under a stream of N$_2$, and left under reduced pressure for a minimum of 2 hours to remove all traces of the organic solvent. The film was resuspended in Hepes buffer by vortexing to a concentration of 2 m$M$. The suspension was then extruded through polycarbonate membranes at 30°C, above the DMPG gel-to-fluid phase transition.[26] The extrusion final step consisted in the use of 0.1-$\mu$m pore diameter polycarbonate membranes, resulting in large unilamellar vesicles (LUVs).

### Measurements

Optical absorption measurements were performed using an HP 8452 A diode array spectrophotometer. For steady-state fluorescence experiments, we employed a Fluorolog 3 Jobin Yvon–Spex spectrometer. Excitation and emission slits of 1- or 2-nm bandpass were used depending on the fluorescence intensity of the sample. The steady-state fluorescence anisotropy was measured at a wavelength emission of 418 nm, with excitation in 310 nm, using Glan Taylor polarizers in an L-format configuration. The values of the fluorescence anisotropy were the averages of three measurements. The temperature was controlled with a refrigerated circulating bath.

Time-resolved experiments were performed using an apparatus based on the time-correlated single-photon counting method. The excitation source was a Tsunami 3950 Spectra Physics titanium–sapphire laser, pumped by a 2060 Spectra Physics argon laser. The repetition rate of 5-ps pulses was set to 400 kHz using the Pulse Picker 3980 (Spectra Physics). The laser was tuned to give an output at 930 nm, and a third harmonic generator BBO crystal (GWN-23PL Spectra Physics) gave the 310-nm excitation pulse that was directed to an Edinburgh FL900 spectrometer. The emission wavelength was selected by a monochromator and emitted photons were detected by a refrigerated Hamamatsu R3809U microchannel plate photomultiplier. The FWHM of the instrument response function was typically 45 ps, determined with a time resolution of 6.0 ps per channel. Measurements were made using a time resolution of 12 or 24 ps per channel. Software provided by Edinburgh Instruments was used to analyze the decay curves and the adequacy of the exponential decay fitting was judged by inspection of the plots of weighted residuals and statistical parameters such as reduced chi-square.

### Analysis of Peptide–Lipid Interaction

Considering an infinite number of available sites for a ligand, the partition of noninteracting molecules between

the aqueous and lipid phases can be analyzed in a simple manner, just allowing for the volumes of the two phases:

$$K_P \equiv \frac{n_M/V_M}{n_{H_2O}/V_{H_2O}} = \frac{C_M}{C_{H_2O}} \quad (1)$$

where $K_p$ is the so-called partition coefficient, $n_M$ and $n_{H_2O}$ are the numbers of ligand moles in the membrane and water, respectively, and $V_M$ and $V_{H_2O}$ are the membrane and water volumes, respectively. For diluted samples, $V_{H_2O}$ is assumed to be equal to the total sample volume ($V_t$).

Equation (1) can be rewritten as a function of the bound ($P_b$, in the membrane), free ($P_f$ in aqueous medium), and total ($P_t = P_b + P_f$) ligand (peptide) concentration:

$$K_p \equiv \frac{[P_b]}{[P_f]}\frac{V_t}{V_M}; \quad \text{hence} \quad [P_b] = \frac{K_p[P_t]V_M}{(K_pV_M + V_t)} \quad (2)$$

If the molecule (peptide) is a fluorophore, displaying different fluorescence anisotropy values in the aqueous and lipid phases, $A_0$ and $A_{max}$, respectively, the fluorescence anisotropy measured for a given sample will be

$$A = \frac{[P_b]}{[P_t]}A_{max} + \frac{[P_f]}{[P_t]}A_0 \quad (3)$$

Equations (2) and (3) can be put together to yield an expression for the variation of the peptide fluorescence anisotropy as a function of the lipid concentration [$L_t$]:

$$\frac{A}{A_0} = \frac{K_p[L_t]M_w/\rho}{1 + (K_p[L_t]M_w/\rho)}\left(\frac{A_{max}}{A_0} - 1\right) + 1 \quad (4)$$

where $M_w$ and $\rho$ are the lipid molecular weight and density ($\rho$ was assumed to be 1 kg/L), respectively, and the equality $V_M/V_t = [L_t] (M_w/\rho)$ was used.

Alternatively, in the case of a limited number of available sites for noninteracting ligands in the membrane, the ligand/macromolecule binding model that leads to the Scatchard equation can be used[27]:

$$\frac{[L_b]/[M_t]}{[L_f]} = \frac{m}{k} - \frac{[L_b]/[M_t]}{k} \quad (5)$$

but adapted to the peptide membrane/aqueous partition problem: [$L_b$] and [$L_f$], are, respectively, changed to [$P_b$] and [$P_f$]; the total macromolecule concentration, [$M_t$], is changed to total amphiphilic aggregates concentration (vesicles or micelles), [Agg$_t$]; $m$ becomes the number of available sites in the aggregate (and not in the macromolecule); and $k$ is the microscopic dissociation constant for the peptides in the aggregates. Considering that $N_0$, the number of lipids per aggregate (vesicle), can be written as $N_0 = mn$, where $n$ is the number of lipids per binding site,

$$[L_b]/[M_t] \equiv [P_b]/[\text{Agg}_t] \equiv [P_b]/([L_t]/N_0)$$

Therefore, Eq. (5) can be written as

$$\frac{[P_b]N_o}{[L_t][P_f]} = \frac{m}{k} - \frac{[P_b]N_o}{[L_t]k}$$

and considering $N_0 = mn$

$$\frac{[P_b]}{[L_t][P_f]} = \frac{1}{nk} - \frac{[P_b]}{[L_t]k} \quad (6)$$

As expected, the final Eq. (6) does not depend on $N_0$ or $m$, as the problem considered here is the partitioning of a molecule into two phases, a lipid and an aqueous phase, with the former having a limited number of available sites. Taking that equation together with Eq. (3), it is possible to write an expression for the variation of the peptide fluorescence anisotropy as a function of the total concentration of lipids for a limited number of available sites in a membrane:

$$\frac{A}{A_0} = \frac{((A_{max}/A_o) - 1)}{2[P_t]n}\left[b \pm (b^2 - 4[P_t][L_t]n)^{1/2}\right] + 1 \quad (7)$$

where $b = [L_t] + [P_t]n + nk$.

For the usual linear Scatchard plot, Eq. (3) was rewritten as

$$[P_f] = [P_t]\frac{A_{max} - A}{A_{max} - A_0} \quad (8)$$

For each lipid concentration [$L_t$], and the corresponding measured $A$ value, the values of [$P_f$] and [$P_b$] = [$P_t$] − [$P_f$] were calculated. The plotting of [$P_b$]/[$L_t$][$P_f$] v. [$P_b$]/[$L_t$] should be a straight line, allowing the calculation of $k$ and $n$ [Eq. (6)].

## Electrostatic Correction

The electrostatic effect on peptide–membrane interaction can be examined using procedures based on the Gouy–Chapman theory.[28] The binding of positively charged peptides results in a partial neutralization of negatively charged membrane, decreasing the surface charge density and, consequently, the surface potential. The vesicle surface charge density ($\sigma$) is given by[28]

$$\sigma = e_0(z_L X_L + z_p X_b)/a_L(1 + X_b a_p/a_L) \quad (9)$$

where $e_0$ is the elementary charge, $X_L$ is the mole fraction of charged lipids (of charge $Z_L$), $Z_p$ is the charge of the peptide, $a_L$ and $a_p$ are the surface areas of lipid and peptide, respectively, and $X_b$ is $X/0.56$, and $X = [P_b]/[L_t]$. Here, only the outer membrane surface is involved in the electrostatic attraction and the factor 0.56 accounts for the fractional concentration of lipids in the outer surface of the vesicles with a 100-nm diameter.[29] In the calculations, we used 60 $\text{Å}^2$ for $a_L$[30] and −0.6 for $z_L X_L$ to take into account the Na$^+$-PG association constant.[26] The value of $a_p$ used for Abz-BK-NH$_2$ and des-Arg$^9$-BK-DAP(Abz)-NH$_2$ was 200 $\text{Å}^2$ and for Abz-BK$^{1-5}$-NH$_2$ 100 $\text{Å}^2$, following values proposed in the literature.[30]

The surface charge density $\sigma$ generates a surface potential that, in the high potential approximation, can be written as

$$\Psi_0 = -\frac{k_B T}{e_0} \ln \frac{\sigma^2}{2\varepsilon\varepsilon_0 k_B T \sum ci} \qquad (10)$$

where $k_B$ is the Boltzmann constant, $\varepsilon$ is the medium dielectric constant, $\varepsilon_0$ is the permittivity of free space, $\Sigma ci$ is the total bulk ionic strength (in M/L) and $T$ is the absolute temperature. The charged membrane influences the distribution of charged molecules in the medium. The cationic peptide concentration at the membrane surface $[P_m]$ and in the bulk phase $[P_f]$ will be related through the Boltzmann equation:

$$[P_m] = [P_f]e^{-Z_p e_o \Psi_o k_B T} \qquad (11)$$

The concentration of peptides at the membrane surface $[P_m]$ were then used in Scatchard plots [Eq. (6)] to analyze the electrostatic effects in the peptide–membrane interaction.

## RESULTS AND DISCUSSION

### Spectroscopic Properties in Aqueous Solution

The optical absorption and fluorescence emission spectral characteristics of the Abz-labeled BK fragments are similar to those observed for the peptide Abz-BK-NH$_2$.[24] The optical absorption band associated to the $^1A \rightarrow L_b$ transition,[31] which occurs in 310 nm in free Abz in buffer pH 7.4, is also displaced to 316 nm in the fragments Abz-BK$^{1-5}$-NH$_2$ and des-Arg$^9$-BK-DAP(Abz)-NH$_2$. The maximum of the fluorescence emission of the peptides is at 418 nm (Fig-
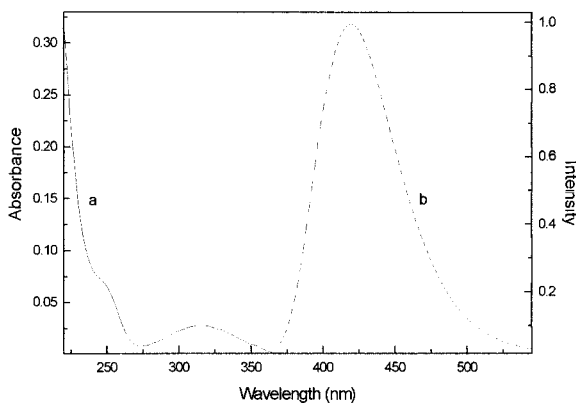


**FIGURE 1** Optical absorption (a) and fluorescence emission (b) spectra of Abz-BK-NH$_2$ ($10^{-5}M$) in Hepes buffer, 0.01$M$, pH 7.4, at 30°C.
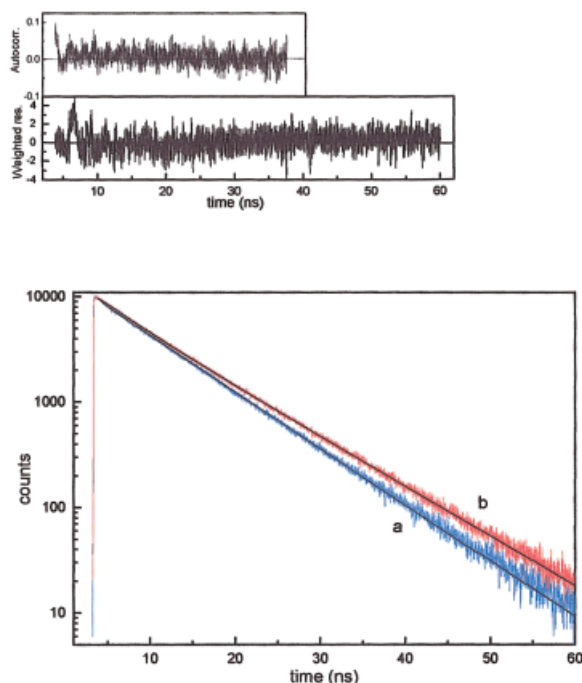


**FIGURE 2** Fluorescence decay curves of Abz-BK-NH$_2$ (a) in aqueous solution and (b) in the presence of 0.5 m$M$ of DMPG at 30°C. The decay was fitted with a double-exponential function (data in Table I). The quality of the fit is indicated by the weighted residual and the autocorrelation function shown in the upper panels.

ure 1), red shifted compared to the emission of free Abz in water, which is located at 396 nm. The binding of Abz to the DAP group in the C-terminal of the peptide des-Arg$^9$-BK-DAP(Abz)-NH$_2$ resulted in spectral characteristics similar to those observed when the fluorophore was bound to the N-terminal of aminoacids and peptides.[19,21]

The time-resolved fluorescence decay of the three peptides was also examined (Figure 2). We observed that in peptides with Abz bound to the N-terminal, Abz-BK-NH$_2$ and Abz-BK$^{1-5}$-NH$_2$, the decay kinetics, in buffer pH 7.4, were practically monoexponential, dominated by lifetimes of 8.03 and 7.99 ns, respectively, accounting for 98% of the total emission (Table I). Those values are smaller than the lifetime of 8.4 ns obtained from the monoexponential decay of free Abz in aqueous solution and comparable to 8.1 ns previously measured for Abz-Arg-NHCH$_3$,[19] indicating some quenching effect in the Abz emission due to its binding to the Arg residue. There was also some contribution (2% of the total emission) from a short lifetime component around 0.50 ns with normalized preexponential factor of circa 0.20 (Table I). The presence of the short component was necessary to adequately fit the experimental decay curve, and sug-

**Table I    Time-Resolved Fluorescence Parameters for the Peptides in Solution and in the Presence of DMPG, in HEPES Buffer, 0.01$M$, pH 7.4, 30°C**

| System | $\tau_1$ (ns) | $\tau_2$ (ns) | $\alpha_1$ | $P_1$ | $\langle \tau \rangle$ | $\chi^2$ |
|---|---|---|---|---|---|---|
| Abz-BK-NH$_2$ | 8.03 | 0.46 | 0.79 | 98 | 7.95 | 1.09 |
| + 0.5 m$M$ DMPG | 9.24 | 4.52 | 0.79 | 89 | 8.72 | 0.99 |
| Abz-BK$^{1-5}$-NH2 | 7.99 | 0.56 | 0.82 | 98 | 7.87 | 1.07 |
| + 0.5 m$M$ DMPG | 8.81 | 4.25 | 0.78 | 88 | 8.27 | 1.06 |
| des-Arg$^9$-BK-DAP(Abz)NH$_2$ | 8.52 | 3.72 | 0.85 | 93 | 8.16 | 1.04 |
| + 0.5 m$M$ DMPG | 9.64 | 4.75 | 0.76 | 87 | 9.02 | 0.98 |

$\tau_i$, fluorescence lifetimes; $\alpha_1$, normalized preexponential factor for the long component; $P_1$ percentile contribution of the long component; $\langle \tau \rangle$, mean lifetime. Excitation wavelength was 316 nm and emission 418 nm. The standard errors in the values of $\tau$ and $\alpha$ were 0.01 ns and 0.01, respectively. The $\chi^2$ values for the fits are also shown.

gests that part of the fluorophore population is subjected to a different quenching process. A mean lifetime $\langle \tau \rangle$ for the decay was calculated as a simple weighted average value, from the individual lifetimes $\tau_i$, and the corresponding normalized preexponential factors $\alpha_i$. The values obtained for Abz-BK-NH$_2$ and Abz-BK$^{1-5}$-NH$_2$ were slightly below 8.0 ns, a typical value for Abz bound to amino acids and peptides.[19,21] The decay of the peptide having Abz bound to the C-terminal, des-Arg$^9$-BK-DAP(Abz)-NH$_2$, was dominated by a long lifetime of 8.52 ns, with some contribution (7% of the total emission) from a 3.72-ns component (Table I). The calculated mean lifetime was 8.16 ns, higher than those found for the two other peptides, indicating that Abz bound to diaminopropi-

onic acid is not affected by the quenching effects present when Abz is bound to the Arg residue.

The steady-state anisotropy of Abz in aqueous solution was 0.005 ± 0.005, and the time-resolved anisotropy decay was fitted to a monoexponential function with rotational correlation time equal to 44 ps, indicating a fast and isotropic movement for the molecule in aqueous medium. The three peptides in buffer presented low and similar values for the steady-state anisotropy, around 0.012 ± 0.005.

At least two exponentials were required to fit the data for the time-resolved anisotropy decay (Figure 3 and Table II): one short time ranging from 46–113 ps, and a longer one, between 330 and 420 ps. Biexponential anisotropy decay is commonly observed in
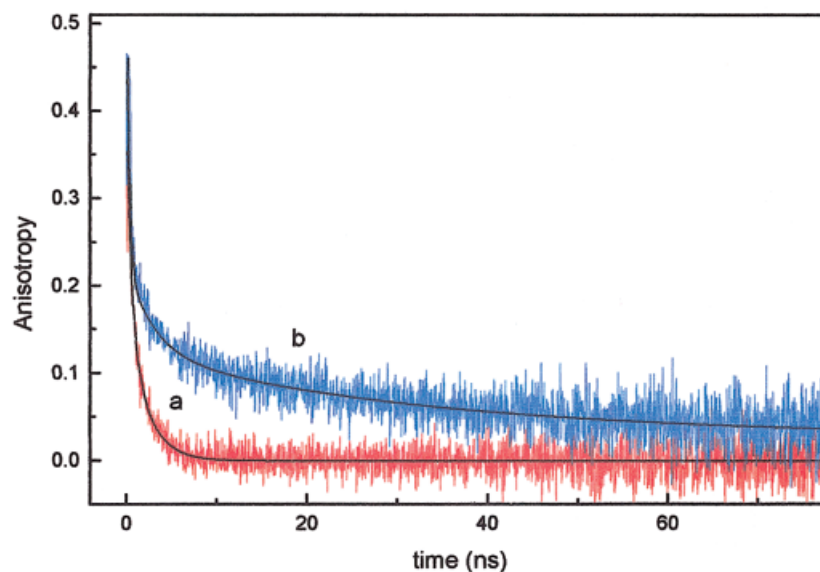


**FIGURE 3**    Fluorescence anisotropy decay of Abz-BK$^{1-5}$-NH$_2$ (a) in aqueous solution and (b) in the presence of 0.9 m$M$ of DMPG at 30°C. Excitation and emission wavelengths were 310 and 420 nm, respectively. The decay was fitted with a double-exponential function (data in Table II).

**Table II**    (*A*) **Steady-State Anisotropy (φ_i) Rotational Correlation Times, and (α_i) Preexponential Factors for the Peptides in Solution and in the Presence of DMPG, in HEPES Buffer, 0.01M, pH 7.4, 30°C**

| System | $A$ | $\phi_1$ (ns) | $\phi_2$ (ns) | $\alpha_1$ | $\alpha_2$ | $\chi^2$ |
|---|---|---|---|---|---|---|
| Abz-BK-NH$_2$ | 0.013 | 0.113 ± 0.015 | 0.42 ± 0.04 | 0.190 | 0.126 | 0.986 |
| +DMPG [0.64 m*M*] | 0.129 | 0.36 ± 0.03 | 6.93 ± 0.45 | 0.126 | 0.124 | 1.080 |
| Abz-BK$^{1-5}$-NH$_2$ | 0.012 | 0.065 ± 0.01 | 0.33 ± 0.02 | 0.162 | 0.170 | 1.016 |
| + DMPG [0.92 m*M*] | 0.084 | 0.23 ± 0.01 | 4.25 ± 0.20 | 0.128 | 0.095 | 1.045 |
| des-Arg$^9$-BK-DAP(Abz)NH$_2$ | 0.011 | 0.046 ± 0.01 | 0.34 ± 0.03 | 0.225 | 0.161 | 0.972 |
| +DMPG [0.5 m*M*] | 0.091 | 0.14 ± 0.02 | 4.2 ± 0.3 | 0.114 | 0.095 | 1.066 |

Errors in preexponential factors ($\alpha_i$) ranged between 5 and 10%.

peptides and proteins, and the short correlation time is usually ascribed to the local probe motion while the long correlation time is related to the overall tumbling of the whole peptide.[24,32] Considering that both short and long correlation times were longer for Abz bound to BK, it seems that, in the native hormone, the local movement is slower and the peptide as a whole is also tumbling slightly slower, as expected for a larger molecule compared with the fragments.

## Spectroscopic Properties in Lipid Medium

Experiments on the interaction of peptides with lipids were carried out adding small amounts of concentrated lipid vesicle dispersion to the peptide solution, maintaining the peptide concentration approximately constant ($10^{-5}M$). At lipid concentrations such that the peptides supposedly were completely bound to DMPG vesicles (see titration curves as discussed below), we observed that the fluorescence emission spectrum of Abz-BK-NH$_2$ was shifted to lower wavelengths (412 nm). The change in the spectral position can be attributed to transfer of Abz from the aqueous medium to the vesicle hydrophobic microenvironment, similar to that observed for the intrinsic fluorescent probe tryptophan, present, for instance, in melanotropins.[33,34] The results are in agreement with measurements made with Abz-BK-NH$_2$ in trifluoroethanol and ethanol, solvents less polar than water, where a blue shift was observed in the Abz emission spectrum.[24] A same blue shift was also observed in the interaction of Abz-BK-NH$_2$ with anionic micelles of SDS (results not shown).

The decay kinetics of the peptides in the presence of lipid vesicles was also best fitted to a biexponential function (Table I) and the preexponential factors in water and lipid media were similar, indicating the absence of interconversion between the two different

species that could be originating the different lifetimes. For all peptides, the Abz longer lifetime $\tau_1$ slightly increased in the presence of lipid vesicles. Moreover, for Abz-BK-NH$_2$ and Abz-BK$^{1-5}$-NH$_2$ the short lifetime raised significantly, from 0.5 to more than 4.0 ns. The short lifetime for des-Arg$^9$-BK-DAP(Abz)-NH$_2$ was already relatively large in aqueous solution (3.72 ns), so only a small increase to 4.75 ns was observed in the presence of DMPG vesicles. The long lifetime for this BK fragment attained the highest value among the peptides studied. Hence, for the three peptides studied here the Abz mean lifetime increased in the presence of lipid vesicles and that increase, compared to the values obtained in aqueous solution, suggests the peptides' penetration into the lipid bilayer, which would reduce the nonradiative decay process driven by the fluorophore–water interaction.

The steady-state fluorescence anisotropy (*A*) of the Abz-labeled peptides in the presence of saturating amount of lipids showed a significant increase compared with the values measured in aqueous solution. We observed an increase from 0.012 presented by the peptides in water to 0.129 for Abz-BK-NH$_2$, 0.091 for des-Arg$^9$-BK-DAP(Abz)-NH$_2$, and 0.084 for Abz-BK$^{1-5}$-NH$_2$ in the presence of DMPG vesicles (Table II). Therefore, the anisotropy data also indicates that the Abz group inserts into the membrane, having its mobility significantly reduced. It is interesting to point out that the restriction to movement is more pronounced in the labeled native peptide Abz-BK-NH$_2$ as compared to the fragments, suggesting a more effective interaction of the labeled native peptide with the lipid vesicles.

Typical anisotropy decay of Abz-BK$^{1-5}$-NH$_2$ in solution and in the presence of DMPG vesicles are shown in Figure 3. The parameters resulting from the fits to exponential curves are presented in Table II for the three peptides in the presence of a lipid saturating

concentration and compared with the values obtained in aqueous solution. Like in aqueous solution, in the presence of DMPG the anisotropy decays were also best fitted to biexponential functions, but with a significant increase in both short and long rotational correlation times. For Abz-BK-NH$_2$ in the presence of 0.65 m$M$ of DMPG, we observed an increase in the short component (113 ps in solution and 360 ps in DMPG) and a more significant increase in the long component (0.42 ns in solution and 6.93 ns in DMPG). As mentioned before, the biexponential anisotropy decay is interpreted as resulting from the local motion of the probe (fast decay component) and the overall tumbling of the whole peptide (slow decay component). The results in the presence of lipid vesicles can also be compared to the values of 280 ps and 1.34 ns of the short and long rotational correlation times, respectively, obtained for Abz-BK-NH$_2$ in trifluoroethanol,[24] a solvent with viscosity significantly higher than that of water. Thus, the increase in both rotational correlation times is consistent with the insertion of the probe in the viscous environment of the lipid bilayer. That increase for Abz bound to the fragments was also significant but less pronounced than observed in Abz-BK-NH$_2$. This result is in accord with that obtained with steady-state fluorescence anisotropy, suggesting that Abz-BK-NH$_2$ penetrates deeper in the bilayer than the fragments. It is also possible that electrostatic effects contribute to the higher degree of restriction to movement of that peptide. The interaction of the negative charges of the vesicle surface with the two positively charged Arg residues of Abz-BK-NH$_2$ should be stronger than the interaction with the single charged fragments.

## Peptide Aqueous/Membrane Partition

To measure the peptide partition into the lipid phase, small amounts of a concentrated lipid vesicle suspension were added to the peptide solution and changes in different Abz fluorescence parameters were examined, like spectral position, intensity, anisotropy, and
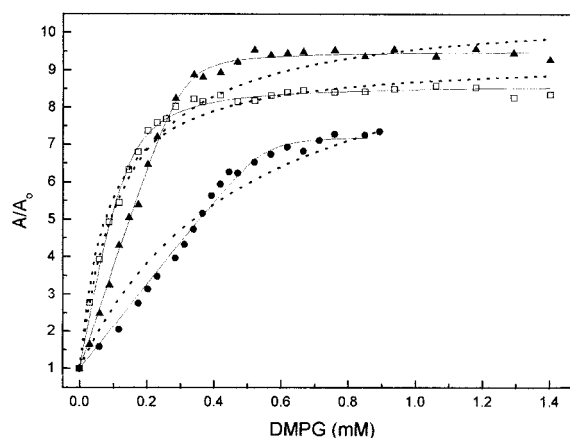


**FIGURE 4** Relative increase in fluorescence anisotropy of (▲) Abz-BK-NH$_2$, (□) des-Arg$^9$-BK-DAP(Abz)-NH$_2$, and (●) Abz-BK$^{1-5}$-NH$_2$ in the presence of DMPG vesicles. Excitation is at 316 nm and emission fixed at 420 nm. Peptide concentration $10^{-5}M$, in 0.01$M$ Hepes buffer, pH 7.4, 30°C. $A_0$ represents the fluorescence anisotropy without lipid. The lines represent the theoretical fittings obtained with Eq. (4), broken lines, and Eq. (7), solid lines.

lifetime. Among them, we chose to monitor the lipid–peptide interaction by following the changes in the steady-state fluorescence anisotropy of Abz, as this parameter gave the most reproducible results. The experimental lipid titration curves for the three peptides are presented in Figure 4. They were analyzed considering the two models discussed in Materials and Methods. The best fittings (applying a least-square procedure) obtained considering an infinite number of available sites for the peptides in the membrane [broken lines in Figure 4 correspond to Eq. (4)] are obviously distant from the experimental data for the three peptides. However, the data could be well fitted with Eq. (7) (solid lines in Figure 4), which models a membrane with a restricted number of available sites. The number of bound lipids per peptide (the size of the binding site) and the microscopic

**Table III    Binding Parameters of Peptides to DMPG Vesicles in 0.01$M$ Hepes Buffer, pH 7.4, 30°C**

| Peptides | Fit Eq. (7) | | Scatchard Plot | | Scatchard Corrected[a] | |
|---|---|---|---|---|---|---|
| | $k$ ($\mu M$) | $n$ | $k$ ($\mu M$) | $n$ | $k$ (m$M$) | $n$ |
| Abz-BK-NH$_2$ | 0.18 ± 0.05 | 17 ± 1 | 0.15 ± 0.02 | 17 ± 1 | 220 ± 20 | 17 ± 1 |
| des-Arg$^9$-BK-DAP(Abz)-NH$_2$ | 1.1 ± 0.3 | 7 ± 1 | 0.9 ± 0.3 | 8 ± 1 | 1.3 ± 0.4 | 7 ± 1 |
| Abz-BK$^{1}$-5-NH2 | 0.09 ± 0.07 | 30 ± 2 | 0.25 ± 0.11 | 26 ± 2 | 0.49 ± 0.5 | 26 ± 2 |

Results obtained from fit to Eq. (7) and from Scatchard plot Eq. (6).

[a] Electrostatic corrected values were obtained from the Scatchard plot, making the corrections presented in Eqs. (8), (9), and (10).
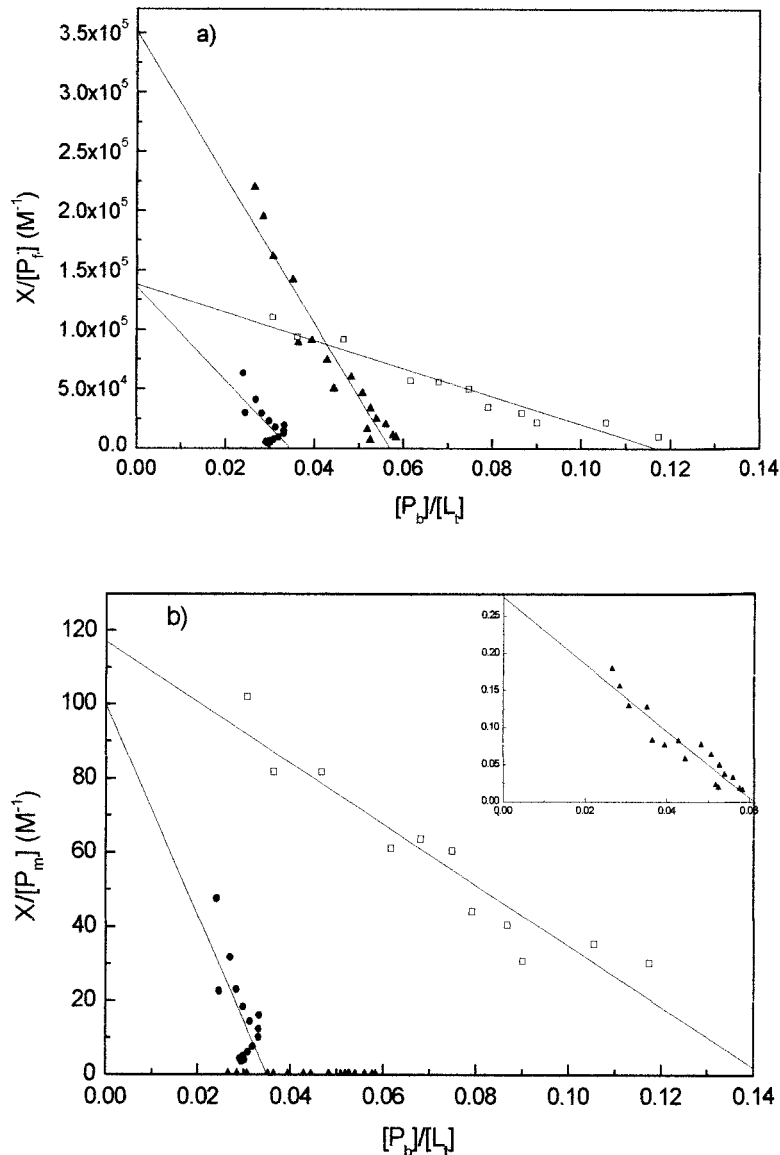
**FIGURE 5** Scatchard plot ($X/[L_t]$ vs $[P_b]/[L_t]$, where $X = [P_b]/[P_f]$), for the binding of (▲) Abz-BK-NH$_2$, (□) des-Arg$^9$-BK-DAP(Abz)-NH$_2$, and (●) Abz-BK$^{1-5}$-NH$_2$ to DMPG vesicles in $0.01M$ Hepes buffer, pH 7.4, 30°C (a). Plots in (b) ($X = [P_m]/[P_f]$) are from concentrations corrected for electrostatic interactions. The inset allows better visualization of data for Abz-BK-NH$_2$ (▲).

dissociation constant are presented in Table III for the three peptides.

The fitting according to Eq. (7) can be compared to the usual linear Scatchard plot (see Material and Methods). The values of the dissociation constant and the number of lipids bound per peptide determined from the plot of $X/[L_t]$ vs. $[P_b]/[L_t]$, where $X = [P_b]/[P_f]$ [Figure 5(a)], are comparable to those resulting from the fitting of the titration curves (Table III). Large uncertainties are present in the dissociation constants for Abz-BK$^{1-5}$-NH$_2$ obtained from both procedures.

From the values of $k$ and $n$, we can observe that the fragment des-Arg$^9$-BK-DAP(Abz)-NH$_2$ presents the higher dissociation constant (lower membrane affinity) and the affinities of the two other peptides for DMPG vesicles are roughly similar. However, the number of lipid molecules involved in the interaction with the small fragment is much higher than the values obtained for the other peptides (see Table III). This is contrary to the expectation that a smaller number of lipid molecules should be interacting with the small peptide, a result that merits further investigation.

## Electrostatic Effects

The electrostatic effect on the binding of Abz-BK-NH$_2$ (with two positives charges), des-Arg$^9$-BK-DAP(Abz)-NH$_2$, and Abz-BK$^{1-5}$-NH$_2$ (both with only one positive charge) to DMPG was examined using procedures based on the Gouy–Chapman theory,[28] largely employed in the literature to evaluate the electrostatic effect on the binding of charged peptides to acidic lipids[33–36] and explained in Materials and Methods.

As for uncorrected data, Scatchard analysis was performed taking into account electrostatic effects using the concentration of peptides at the membrane surface [$P_m$] calculated according to Eqs. (9), (10) and (11). The use of [$P_m$] instead of [$P_f$] means that the binding of the peptides to the membrane is determined considering the interaction between lipids in the bilayer and peptides accumulated near to the vesicle surface due to the electrostatic effects. The net charge considered in the calculations was $-1$ for lipids, $+2$ for Abz-BK-NH$_2$, and $+1$ for the BK fragments, des-Arg$^9$-BK-DAP(Abz)-NH$_2$ and Abz-BK$^{1-5}$-NH$_2$.

The values of $k$ and $n$ obtained from electrostatic corrected Scatchard plots [Figure 5(b)] for the fragments with net charge $+1$ are three orders of magnitude higher than those calculated without considering the electrostatic effects (Table III). However, the number of bound lipids per peptide, $n$, is not affected by the electrostatic correction that accounts just for the increase in the concentration of peptides close to the surface of the vesicles. Therefore, the awkward large number of bound lipids obtained for the fragment Abz-BK$^{1-5}$-NH$_2$ does not change with electrostatic corrections only.

Electrostatic interaction is responsible for the increase in the concentration of cationic peptides near the surface of anionic vesicles and the effect should be more pronounced for Abz-BK-NH$_2$, which has two positive charges. In fact, in Figure 5(b) the numbers for Abz-BK-NH$_2$ in the vertical axis are two orders of magnitude lower than those for the other peptides. Despite this, the inset in Figure 5(b) shows that the plot for the native peptide is linear. The value of the corrected dissociation constant is higher for that peptide compared to the results obtained for the labeled fragments that present charge $+1$. Thus, corrections for the changes in peptide concentration due to electrostatic interactions lead to indications of higher affinity of the fragments to the hydrophobic phase of the bilayer. The effective charge of BK could possibly be lower than $+2$, as found for other cationic peptides, but even using a somewhat smaller nominal charge the Abz-BK-NH$_2$ lipid affinity is still lower than that

presented by the fragments. For example, using a charge of $+1.5$ for BK the dissociation constant is 6.78 m$M$, still higher than the values obtained for the fragments.

## CONCLUSIONS

In this articles we examined BK and derived peptides labeled with the fluorescent probe Abz. In BK and BK$^{1-5}$, the probe was bound to the nitrogen atom from the amino terminal group of the peptide, while in des-Arg$^9$-BK it was bound to the amino nitrogen of the DAP group attached to the carboxy terminal of the peptide. In both cases, we observed that the absorption band of the free probe in water solution shifted from 310 to 316 nm and the fluorescence emission displaced from 396 to 420 nm. In aqueous solutions, lifetimes for the probe in the three peptides were also similar, around 8.0 ns. Steady-state anisotropy gave information about rotational movement of the probe and the peptide as a whole, and no differences could be detected among the peptides in water solution. From time-resolved anisotropy, we verified that Abz bound to the native hormone has a somewhat slower movement than that bound to the fragments. The results as a whole indicated that the general spectral characteristics of the probe seem independent of the binding position in the peptide chain.

Interaction of the labeled peptides with DMPG vesicles was ascertained by examination of emission peak displacements, changes in lifetime, and anisotropy upon addition of vesicles to the peptide solution. The increase in steady-state anisotropy and rotational correlation times obtained from anisotropy decay profiles are more pronounced for Abz-BK-NH$_2$. Within experimental errors, anisotropy results for the two fragments are similar, indicating that they present higher mobility in the membrane compared with the labeled native peptide. Taking into account the corrections due to the vesicle surface potential, and, consequently, to the peptide concentration near the vesicles, the dissociation constant is higher for Abz-BK-NH$_2$ than for the fragments. Compared to Abz-BK-NH$_2$, the lipid–water partition equilibrium of the labeled fragments is more effectively displaced to the hydrophobic phase of the bilayer.

The fluorescence measurements indicated that the three peptides studied here penetrate into the lipid phase of DMPG vesicles and that is certainly related to the changes in the membrane fluidity observed using ESR probes.[14] It is interesting to note that fluorescence experiments detect differences in the behavior of the peptides interacting with the fluid phase

of DMPG vesicles, which were not observed using ESR to monitor the effects of the interaction in the membrane fluidity. The greater affinity of the B2-type receptor for BK can be associated to regions of the protein with negative charges, increasing the degree of interaction of the hormone. The loss of Arg[9] residue reduces the electrostatic effects and favoring the interaction with hydrophobic regions of the B1-type receptor, can contribute to the consequent receptor selectivity to that fragment.

## REFERENCES

1. Mason, D. T.; Melmon, K. L. J Clin Invest 1966, 45, 1685–1699.
2. Regoli, D.; Barabé, J. Pharmacol Rev 1980, 32, 1–46.
3. Proud, D.; Reynolds, C. J.; Lacapra, S.; Kagey-Sbotka, A.; Lichtenstein, L. M.; Naclerio, R. M. Am Rev Respin Dis 1988, 137, 613–616.
4. Stewart, J. M. Biopolymers 1995, 37, 143–155.
5. Regoli, D.; Suzanne, N. A.; Rizzi, A.; Gobeil, F. J. Eur J Pharmacol 1998, 348, 1–10.
6. Stewart, J. M.; Gera, L.; Hanson, W.; Zuzack, J. S.; Burkard, M.; McCullough, R.; Whalley, E. T. Immunopharmacology 1996, 33, 51–60.
7. Cann, J. R.; Stewart, J. M.; Matsueda, G. R. Biochemistry 1973, 12, 3780–3788.
8. Denys, L.; Bothner-By, A. A.; Fisher, G. H.; Ryan, J. W. Biochemistry 1982, 21, 6531–6536.
9. Cann, J. R.; Liu, X.; Stewart, J. M.; Gera, L.; Kotovych, G. Biopolymers 1994, 34, 869–878.
10. Lee, S. C.; Russel, A. F.; Laidig, W. D. Int J Peptide Protein Res 1990, 35, 367–377.
11. Pellegrini, M.; Mammi, S.; Peggion, E.; Mierke, D. F. J Med Chem 1997, 40, 92–98.
12. Young, J. K.; Graham, W. H.; Beard, D. J.; Hicks, R. P. Biopolymers 1992, 32, 1061–1064.
13. Kotovych, G.; Cann, J. R.; Stewart, J. M.; Yamamoto, H. Biochem Cell Biol 1998, 76, 257–266.
14. Turchiello, R. F.; Juliano, L.; Ito, A. S.; Lamy-Freund, M. T. Biopolymers 2000, 54, 211–221.
15. Sargent, D. F.; Schwyzer, R. Proc Natl Acad Sci USA 1986, 83, 5774–5778.
16. Schwyzer, R. Biochemistry 1986, 25, 6335–6341.
17. Rao, A. G.; Stewart, J. M.; Vavrek, R. J.; Sillerud, L. O.; Fink, N. H.; Cann, J. R. Biochim Biophys Acta 1989, 997, 278–283.
18. Melhuish, W. H. J Phys Chem 1961, 65, 229–235.
19. Ito, A. S.; Turchiello, R. F.; Hirata, I. Y.; Cezari, M. H.; Meldal, M.; Juliano, L. Biospectroscopy 1998, 4, 395–402.
20. Hirata, I. Y.; Sedenho, M. H. C.; Boschcov, P.; Garratt, R. C.; Oliva, G.; Ito, A. S.; Spisni, A.; Franzoni, L.; Juliano, L. Lett Peptide Sci 1998, 5, 1–10.
21. Turchiello, R. F.; Lamy-Freund, M. T.; Hirata, I. Y.; Juliano, L.; Ito, A. S. Biophys Chem 1998, 73, 217–225.
22. Chagas, J. R.; Portaro, F. C.; Hirata, I. Y.; Almeida, P. C.; Juliano, M. A.; Juliano, L.; Prado, E. S. Biochem J 1995, 306, 63–69.
23. Del Nery, E.; Chagas, J. R.; Juliano, M. A.; Prado, E. S.; Juliano, L. Biochem J 1995, 312, 233–238.
24. Souza, E. S.; Hirata, I. Y.; Juliano, L.; Ito, A. S. Biochim Biophys Acta 2000, 1474, 251–261.
25. Hope, M. I.; Bally, M. B.; Weeb, G.; Cullis, P. R. Biochim Biophys Acta 1985, 812, 55–65.
26. Riske, K. A.; Amaral, L. Q.; Lamy-Freund, M. T. Biochim Biophys Acta 2001, 1511, 297–308.
27. Cantor, C. R.; Schimmel, P. R. Biophysical Chemistry, Part III; W. H. Freeman and Co.; San Francisco, 1980; Chapter 15.
28. McLaughlin, S. Curr Topics Membr Transp 1977, 9, 71–144.
29. Beschiaschvilli, G.; Seelig, J. Biochemistry 1990, 29, 52–58.
30. Cullis, P. R.; Hope, M. J. In Vance, D. E.; Vance, J. E., Eds. Biochemistry of Lipids and Membranes; Benjamin/Cummings: Menlo Park, CA, 1985, pp. 25–72.
31. Siemion, I. Z.; Wieland, T. Tetrahedron 1977, 33, 155–157.
32. Kulinski, T.; Visser, J. W. G.; O'Kane, D. J.; Lee, J. Biochemistry 1987, 26, 540–549.
33. Ito, A. S.; Castrucci, A. M. L.; Hruby, V. J.; Hadley, M. E.; Krajcarsk, D. T.; Szabo, A. G. Biochemistry 1993, 32, 12264–12272.
34. Macedo, Z. S.; Furquim, T. A.; Ito, A. S. Biophys Chem 1996, 59, 193–202.
35. Seelig, A.; MacDonald, P. M. Biochemistry 1989, 28, 2490–2496.
36. Beschiaschvilli, G.; Seelig, J. Biochemistry 1990, 29, 52–58.